Single-Mode Monolithic Quantum-Dot VCSEL in 1.3 μm With Sidemode Suppression Ratio Over 30 dB

Y. H. Chang, P. C. Peng, W. K. Tsai, Gray Lin, FangI Lai, R. S. Hsiao, H. P. Yang, H. C. Yu, K. F. Lin, J. Y. Chi, S. C. Wang, and H. C. Kuo

***Abstract*—We present monolithic quantum-dot vertical-cavity surface-emitting lasers (QD VCSELs) operating in the 1.3-μm optical communication wavelength. The QD VCSELs have adapted fully doped structure on GaAs substrate. The output power is $\sim$330 μW with slope efficiency of 0.18 W/A at room temperature. Single-mode operation was obtained with a sidemode suppression ratio of $>$30 dB. The modulation bandwidth and eye diagram in 2.5 Gb/s was also presented.**

***Index Terms*—Bandwidth, quantum dots (QDs), single mode, surface-emitting laser.**

I. Introduction

VERTICAL-CAVITY surface-emitting lasers (VCSELs) at around 1.3 μm fabricated on GaAs substrates have been expected to realize high-performance and low-cost light sources for fiber-optic communication systems. The large conduction band offset improves the temperature performance over that of conventional InP-based materials. The GaAs system provides high-performance AlGaAs–GaAs distributed Bragg reflector (DBR) mirrors and permits the use of the well-established oxide-confined GaAs-based VCSEL manufacturing infrastructure. So far, the most promising materials at 1.3 μm on GaAs substrate were GaInAsN quantum wells [1]–[3] and quantum dots (QDs) [4]–[6]. Each of these solutions offers some advantages over its counterpart, but further extending the emission wavelength is relatively easier in QDs than GaInAsN. QD edge-emitting lasers have also been proven to exhibit excellent performance characteristics, including low threshold current, temperature insensitive threshold current, and high differential gain. For VCSELs, QDs [7] are particularly advantageous, as nonequilibrium carriers are localized in the QDs and, thus, spreading of nonequilibrium carriers out of the injection region can be suppressed. This may result in ultralow threshold currents at ultrasmall apertures [7], [8].

Recently, 1.3-μm QD VCSELs using intracavity structures have been proposed [9], [10]. However, devices with a monolithic structure are always desirable. In this letter, we demonstrate monolithically single-mode QD VCSELs with high sidemode suppression ratio (SMSR $>$30 dB) and report the temperature performance and dynamic properties including bandwidth and eye diagram.

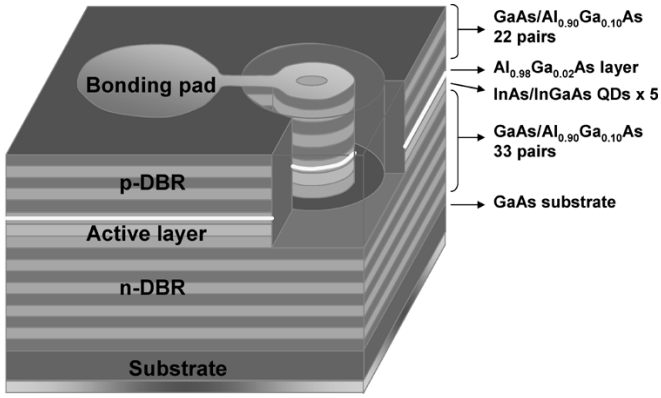

Fig. 1. QD VCSELs device structure.

II. Experiment

All structures were grown on GaAs (100) substrates using molecular beam epitaxy by NL Nanosemiconductor GmbH (Germany). The epitaxial structure was as follows (from bottom to top): n^+-GaAs buffer, 33.5-pair n^+-$Al_{0.9}Ga_{0.1}As$/n^+-GaAs (Si-doped) DBR, undoped active region, p-$Al_{0.98}Ga_{0.02}As$ oxidation layer, 22-pair p^+-$Al_{0.9}Ga_{0.1}As$/p^+-GaAs DBR (carbon-doped), and p^+-GaAs (carbon-doped) contact layer. The graded-index separate confinement heterostructure active region consisted mainly of five groups of the QD's active region embedded between two linear-graded $Al_xGa_{1-x}As$ ($x = 0$ to 0.9 and $x = 0.9$ to 0) confinement layers. The thickness of the cavity active region was 3λ. Each group of QDs was composed of three QD layers and was situated around the antinode of a standing wave. The wavelength detuning is about 12 nm with gain peak at 1266 nm, and cavity resonance at 1278 nm. Carbon was used as the p-type dopant in the DBR to increase the carrier concentration ($2 - 3 \times 10^{18}$ cm^{-3}). The interfaces of both the p-type and n-type $Al_{0.9}Ga_{0.1}As$–GaAs DBR layers are linearly graded to reduce the series resistance. The optical characteristics of QDs were optimized through PL measurement and structural analysis. The details of the process were fully described in our previous work [11]. The mesa diameter of the fabricated device is 26 μm with a $5 \sim 6$ μm oxide aperture, and the device surface is quasi-planar so that the annular p-contact metal and the bond pad are on the same level. The device structure is shown in Fig. 1. The p-contact was formed by directly depositing Ti–Pt–Au on the upper

Manuscript received November 2, 2005; revised December 28, 2005. This work was supported by the National Science Council, Republic of China, under Contract NSC 94-2752-E-009-007-PAE and Contract NSC 94-2215-E-009-020.

Y. H. Chang, P. C. Peng, W. K. Tsai, F. Lai, S. C. Wang, and H. C. Kuo are with the Department of Photonics and Institute of Electro-Optical Engineering, National Chiao-Tung University, Hsinchu, Taiwan 300, R.O.C. (e-mail: hckuo@faculty.nctu.edu.tw).

G. Lin, R. S. Hsiao, H. P. Yang, H. C. Yu, K. F. Lin, and J. Y. Chi are with Opto-Electronics and System Laboratory, Industrial Technology Research Institute, Hsinchu, Taiwan 310, R.O.C.

Digital Object Identifier 10.1109/LPT.2006.871831

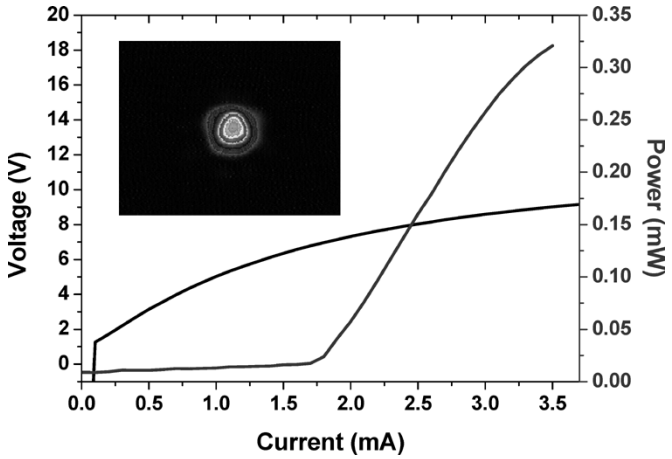

Fig. 2. L–I–V relationship of QD VCSEL. Inset is the near-field pattern of the VCSELs at 3 mA.

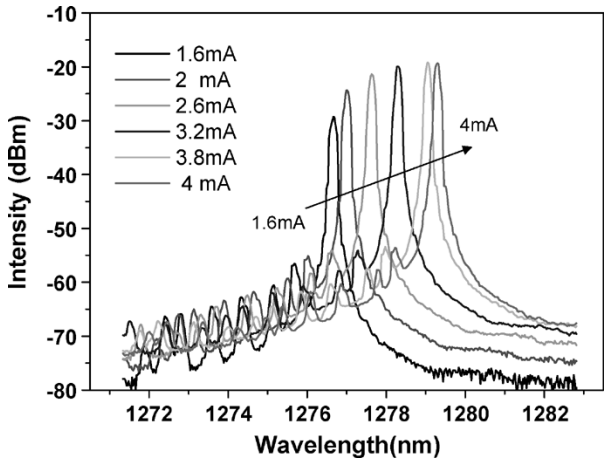

Fig. 3. Emission spectra of QD VCSEL at room temperature.

heavily doped p^+ GaAs contact layer, and Au–Ge–Ni–Au was deposited on the bottom side of the substrate after it had been thinned down. After metal annealing, the sample was immediately probe tested on the wafer level to extract the static operation characteristics.

III. Results and Discussion

The dc characteristics of completed VCSELs were measured using a probe station, an Agilent 4145A semiconductor parameter analyzer, and an InGaAs photodiode. The spectra of the QD VCSELs were measured using an Advantest Q8381A optical spectrum analyzer. Fig. 2 plots curves of light output and voltage versus current (L–I–V). The threshold current is ~1.8 mA and the threshold current density is 7.6 kA/cm^2. The output power rollover occurs as the current increases above 4 mA with maximum optical output of 0.33 mW at 20 °C. In addition, the VCSEL is a single polarization in the full operating range with a ratio of ~20 dB. The inset of Fig. 2 is the near-field pattern of the QD VCSEL biased at 3 mA which indicated the fundamental mode lasing. Fig. 3 shows the typical emission spectra of the QD VCSELs, which indicate single transverse mode operation in the whole operation range with a lasing wavelength of ~1.278 μm and SMSR $>$ 30 dB.

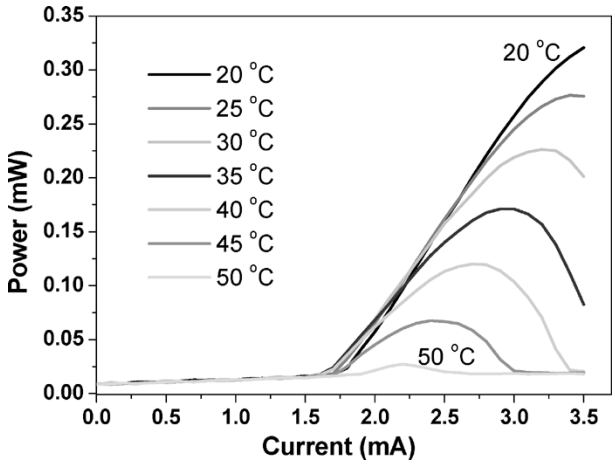

Fig. 4. Temperature-dependent L–I relationship of QD VCSEL.

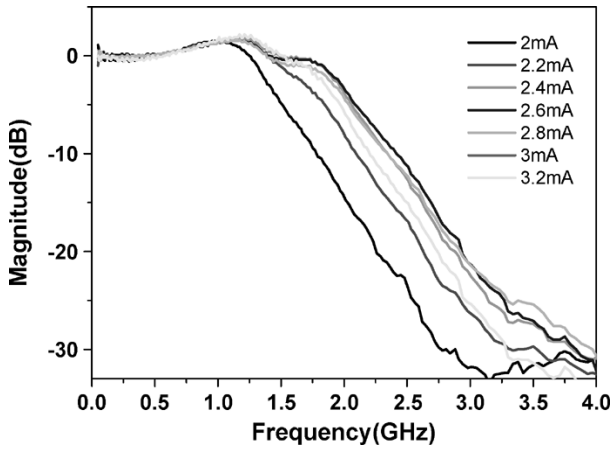

Fig. 5. Small signal modulation response of QD VCSEL.

To investigate the temperature dependence of the QD VCSEL, L–I curves were measured from room temperature to 55 °C with current step of 0.01 mA, as shown in Fig. 4. The threshold current varies only 0.15 mA (<10% of $I_{\rm th}$) with temperatures from 10 °C to 45 °C and the slope efficiency drops from 0.18 to 0.1 W/A. The small temperature dependence of threshold current corresponds to a characteristic temperature (T_0) of 450 K, a high value comparing with the InGaAs(N) VCSEL in 1.3 μm. The high characteristic temperature was attributed to the wide gain spectra of the QD's gain media. When temperature increases, the wide gain spectra make the alignment between gain spectra and cavity resonance not sensitive, and therefore, improves the T_0. However, increase of threshold current with temperature and the quench of output power were also observed after 50 °C which implies the gain of the QDs decreases severely in higher temperature.

The small signal response of VCSELs as a function of bias current was measured at 25 °C using a calibrated vector network analyzer (Agilent 8720ES) with wafer probing and a 50-μm multimode optical fiber connected to a New Focus 25-GHz photodetector. Fig. 5 indicates that the modulation frequency increases with the bias current low current range. At a bias current of larger than 2.5 mA, the bandwidth saturate and the maximum 3-dB modulation frequency response is measured as ~2 GHz. In Fig. 6, the 3-dB bandwidth ($f_{3\ \rm dB}$) is plotted as a function of

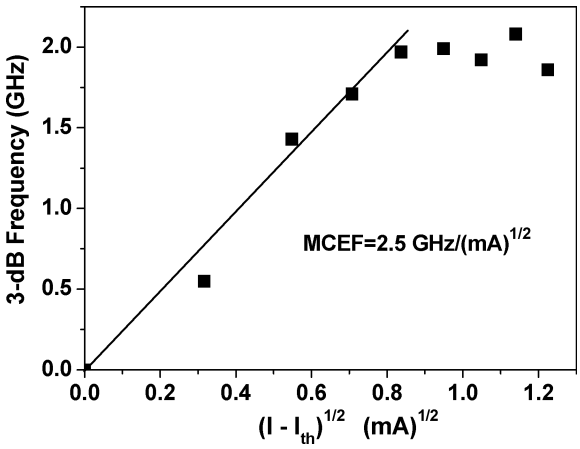

Fig. 6. The 3-dB frequency as a function of square root of current above threshold current.

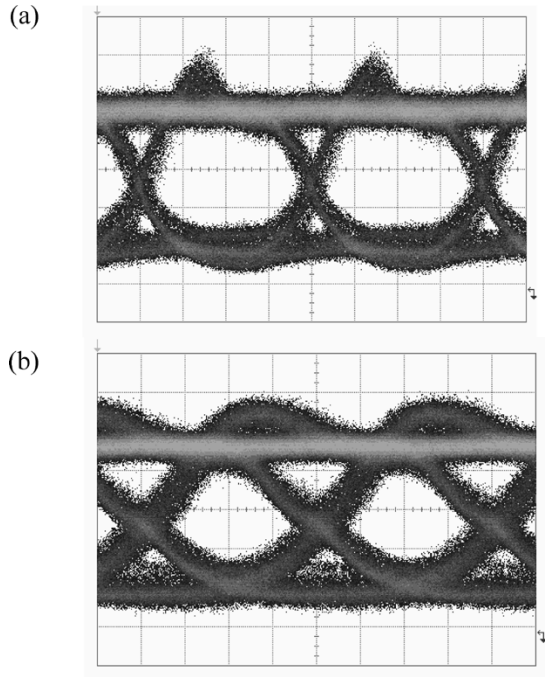

Fig. 7. Eye diagram of the QD VCSELs at (a) 1.25 and (b) 2.5 Gb/s (time scale was 200 and 100 ps/div).

the bias current. At low bias currents, the bandwidth increases in proportion to the square root of the current as expected from the rate equation analysis. The saturation of bandwidth was clearly observed as bias current increases above 2.5 mA which might be attributed to heating effect. Carrier depopulation in QDs subjected to the heated active region may suppress the material gain and put the intrinsic limit of high speed modulation. The modulation current efficiency factor is $\sim 2.5\,\mathrm{GHz}/(\mathrm{mA})^{1/2}$. Improvement can be done by increasing the QD's stacks and reducing the current density of each dot simultaneously. Finally, we illustrate the eye diagram at 1.25 and 2.5 Gb/s (Fig. 7). The QD VCSEL shows a clear and symmetrical eye diagram at 1.25 Gb/s. At 2.5 Gb/s, the eye was degraded due to the overshoot and insufficient bandwidth. Future work will focus on enhancement of high-speed performance by reducing the device parasitic and thermal impedance.

IV. Conclusion

We present monolithic QD VCSELs operating in the 1.3-μm optical communication wavelength. The QD VCSELs have adapted fully doped structure on GaAs substrate. The output power is $\sim$330 μW with slope efficiency of 0.18 W/A at room temperature. Single-mode operation was obtained with SMSR of $>$30 dB.

Acknowledgment

The authors would like to thank Prof. J. H. Chen from National Chiao-Tung University for providing the instruments and technical help.

References

[1] N. Tansu and L. J. Mawst, "Temperature sensitivity of 1300-nm InGaAsN quantum-well lasers," *IEEE Photon. Technol. Lett.*, vol. 14, no. 8, pp. 1052–1054, Aug. 2002.

[2] C. W. Tu and P. Yu, "Material properties of III-V semiconductors for lasers and detectors," *MRS Bull.*, vol. 28, pp. 345–349, 2003.

[3] M. Kawaguchi, T. Miyamoto, E. Gouardes, D. Schlenker, T. Kondo, F. Koyama, and K. Iga, "Lasing characteristics of low-threshold GaInNAs lasers grown by metalorganic chemical vapor deposition," *Jpn. J. Appl. Phys.*, vol. 40, pp. L744–L746, 2001.

[4] S. L. Chuang and N. Holonyak Jr., "Quantum-well assisted tunneling injection quantum-dot lasers," in *Tech. Dig. Conf. Lasers and Electro-Optics*, vol. 1, 2002, p. 297.

[5] T. Yang, J. Tatebayashi, S. Tsukamoto, and Y. Arakawa, "Highly uniform self-assembled InAs/GaAs quantum dots emitting at 1.3 μm by metalorganic chemical vapor deposition," *Physica E*, vol. 26, pp. 77–80, 2005.

[6] N. N. Ledentsov, "Long-wavelength quantum-dot lasers on GaAs substrates: From media to device concepts," *IEEE J. Sel. Topics Quantum Electron.*, vol. 8, no. 5, pp. 1015–1024, Sep./Oct. 2002.

[7] N. N. Ledentsov, M. Grundmann, F. Heinrichsdor, D. Bimberg, V. M. Ustinov, A. E. Zhukov, M. V. Maximov, Z. I. Alferov, and J. A. Lott, "Quantum-dot heterostructure lasers," *IEEE J. Sel. Topics Quantum Electron.*, vol. 6, no. 3, pp. 439–451, May/Jun. 2000.

[8] J. A. Lott, N. N. Ledentsov, V. M. Ustinov, A. Y. Egorov, A. E. Zhukov, P. S. Kop'ev, Z. I. Alferov, and D. Bimberg, "Vertical cavity lasers based on vertically coupled quantum dots," *Electron. Lett.*, vol. 33, pp. 1150–1151, 1997.

[9] J. A. Lott, N. N. Ledentsov, V. M. Ustinov, N. A. Maleev, A. E. Zhukov, A. R. Kovsh, M. V. Maximov, B. V. Volovik, Z. I. Alferov, and D. Bimberg, "InAs-InGaAs quantum dot VCSELs on GaAs substrates emitting at 1.3 μm," *Electron. Lett.*, vol. 36, no. 16, pp. 1384–1385, 2000.

[10] V. M. Ustinov, N. A. Maleev, A. R. Kovsh, and A. E. Zhukov, "Quantum dot VCSELs," *Phys. Status Solidi A*, vol. 202, pp. 396–402, 2005.

[11] H. C. Yu, S. J. Chang, Y. K. Su, C. P. Sung, Y. W. Lin, H. P. Yang, C. Y. Huang, and J. M. Wang, "A simple method for fabrication of high speed vertical cavity surface emitting lasers," *Mater. Sci. Eng. B*, vol. 106, pp. 101–104, 2004.